

## On the electroweak corrections to $t \rightarrow bl^+ \nu_l(\gamma)$ decay

---

**Renat Sadykov\***

*JINR, Dubna (Russia)*

*E-mail: srr@nusun.jinr.ru*

**Andrej Arbuzov**

*JINR, Dubna (Russia)*

*E-mail: arbuzov@thsun1.jinr.ru*

**Dmitry Bardin**

*JINR, Dubna (Russia)*

*E-mail: bardin@nusun.jinr.ru*

**Serge Bondarenko**

*JINR, Dubna (Russia)*

*E-mail: bondarenko@jinr.ru*

**Pena Christova**

*JINR, Dubna (Russia)*

*E-mail: penchris@nusun.jinr.ru*

**Lidia Kalinovskaya**

*JINR, Dubna (Russia)*

*E-mail: kalinov@nusun.jinr.ru*

**Gizo Nanava**

*IFJ, PAN (Poland)*

*E-mail: Gizo.Nanava@ifj.edu.pl*

Radiative corrections to the process of the top quark decay  $t \rightarrow bl^+ \nu_l(\gamma)$  are revisited. Complete one-loop electroweak corrections are calculated within the SANC system. Various distributions are produced by means of Monte Carlo integrator and events generator. Comparison with the results of CompHEP and PYTHIA packages are presented for Born and hard photon contributions.

*International Workshop on Top Quark Physics*

*January 12-15, 2006*

*Coimbra, Portugal*

---

\*Speaker.

## 1. Introduction

The top quark is the only known fundamental fermion with a mass ( $m_t = 178 \pm 4.3$  GeV) on the electroweak scale. For this reason study of the top quark may reveal important information about electroweak symmetry breaking sector of the standard model (SM). One of the aspects of this study is the precision calculation of the decay rates of the top quark. Electroweak (EW) radiative corrections to the process  $t \rightarrow bW^+$  were calculated by several groups [1, 2, 3, 4].

This paper is devoted to the one-loop QED and EW radiative corrections (RC) to the semileptonic top quark decay process  $t \rightarrow bl^+ \nu_l(\gamma)$ . According to the SM the dominant channel of top quark decay is  $t \rightarrow bW^+$  with a branching ratio to be 99.9% [5]. The decay branching ratio of the W-boson into leptons  $Br(W \rightarrow l^+ \nu_l) \approx 11\%$  [6]. Approximately 1/3 part of all top quark decay events is due to the semileptonic ones:  $t \rightarrow bl^+ \nu_l$  ( $l^+ \equiv e^+, \mu^+$  or  $\tau^+$ ).

Here we present the results obtained within the SANC [7] system and some comparisons with the calculation performed by means of CompHEP [8] and PYTHIA [9] packages. Starting from the construction of helicity amplitudes and EW form factors SANC performs calculation of the decay width and produces computer codes which can be further used in the experimental data analysis.

Covariant (CA) and helicity (HA) amplitudes for top and antitop decays were presented in [7]. SANC is also able to compute one-loop QCD corrections [10], however the discussion of this possibility is beyond the scope of this report (see, for example, [11, 12, 13, 14]).

## 2. Calculation scheme

The total one-loop width  $\Gamma^{1\text{-loop}}$  of the decay  $t \rightarrow bl^+ \nu_l(\gamma)$  can be subdivided into four terms:

$$\Gamma^{1\text{-loop}} = \Gamma^{\text{Born}} + \Gamma^{\text{virt}}(\lambda) + \Gamma^{\text{soft}}(\lambda, \bar{\omega}) + \Gamma^{\text{hard}}(\bar{\omega}). \quad (2.1)$$

Here  $\Gamma^{\text{Born}} \equiv \Gamma^{(0)}$  is the decay width in the Born approximation,  $\Gamma^{\text{virt}}$  is virtual contribution,  $\Gamma^{\text{soft}}$  and  $\Gamma^{\text{hard}}$  are the contributions due to the soft and hard photon emission respectively. An auxiliary parameter  $\bar{\omega}$  separates the soft and hard photon contributions and an auxiliary parameter  $\lambda$  ("photon mass") emerges from the virtual contribution and the soft one.

For the numerical calculation we used the next set of input parameters:

$$\begin{array}{lll} m_t = 178 \text{ GeV}, & m_\tau = 1.77699 \text{ GeV}, & \alpha(0) = 1/137.035999, \\ m_b = 4.3 \text{ GeV}, & m_W = 80.425 \text{ GeV}, & G_F = 1.16637 \cdot 10^{-5} \text{ GeV}^{-2}, \\ m_e = 0.000511 \text{ GeV}, & m_Z = 91.1876 \text{ GeV}, & \Gamma_W = 2.138 \text{ GeV}, \\ m_\mu = 0.105658 \text{ GeV}, & m_H = 120 \text{ GeV}, & \Gamma_t = 1.551 \text{ GeV}. \end{array}$$

Electromagnetic coupling  $\alpha = e^2/4\pi$  can be set to different values according to different input parameters schemes. It can be directly identified with the fine-structure constant  $\alpha(0)$ . This choice is called  $\alpha$  scheme. Another value for  $\alpha$  can be deduced from the Fermi constant  $G_F$ . In this case  $\alpha(G_F) = \sqrt{2}G_F m_W^2 \sin^2 \theta_W / \pi$  and this choice is called  $G_F$  scheme. We used both  $G_F$  and  $\alpha$  schemes to produce numbers.

### 3. Born-level process

In the Born approximation there is only one Feynman diagram for decay  $t \rightarrow bl^+ \nu_l$  with one intermediate virtual  $W^+$  boson (see Fig. 1).

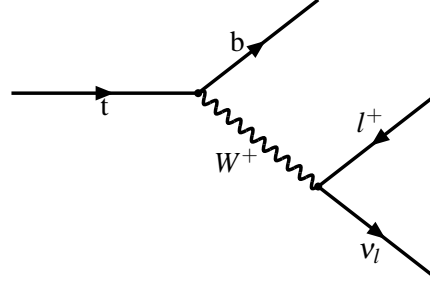


**Figure 1:** Feynman diagram for Born level process.

Differential decay rate in the top quark rest frame:

$$d\Gamma^{\text{Born}} = \frac{1}{2m_t} \sum_{\text{spins}} |\mathcal{M}^{\text{Born}}|^2 d\Phi_3, \quad (3.1)$$

where  $\mathcal{M}^{\text{Born}}$  is an amplitude of the process and  $d\Phi_3$  is the differential three-body phase space. One can express the values  $\mathcal{M}^{\text{Born}}$  and  $d\Phi_3$  via two independent variables:  $s = (p_l + p_\nu)^2$  and  $\cos \theta$ , where  $\theta$  is the angle between  $\vec{p}_l$  and  $\vec{p}_b$  in the rest frame of the compound  $(l^+, \nu_l)$ . After these substitutions were made we obtain:

$$\Gamma^{\text{Born}} = \int_{-1}^1 d\cos \theta \int_{m_l^2}^{(m_t - m_b)^2} ds f(s, \cos \theta). \quad (3.2)$$

The result of two-fold Monte-Carlo integration shown in Tab. 1. This calculation performed by means of Monte-Carlo integration routine based on the VEGAS algorithm [15].

$\Gamma^{\text{Born}}$ (SANC)	$\Gamma^{\text{Born}}$ (CompHEP)	$\Gamma^{\text{Born}}$ (PYTHIA)
0.17303(1) GeV	0.17301(1) GeV	0.16782(1) GeV

**Table 1:** Born-level decay width for the process  $t \rightarrow b\mu^+ \nu_\mu$  produced by SANC and comparison with the results of CompHEP and PYTHIA packages.

The results of SANC and CompHEP are in fair agreement, the deviation from PYTHIA appears due to the difference in the definition of EW constants. In addition to integration we used Monte-Carlo events generator of unweighted events to produce differential distributions. In Fig. 2 we presented some of these distributions and comparison with distributions, obtained with the help of CompHEP and PYTHIA packages. We note, that the input parameters for this comparison were tuned between SANC and CompHEP.

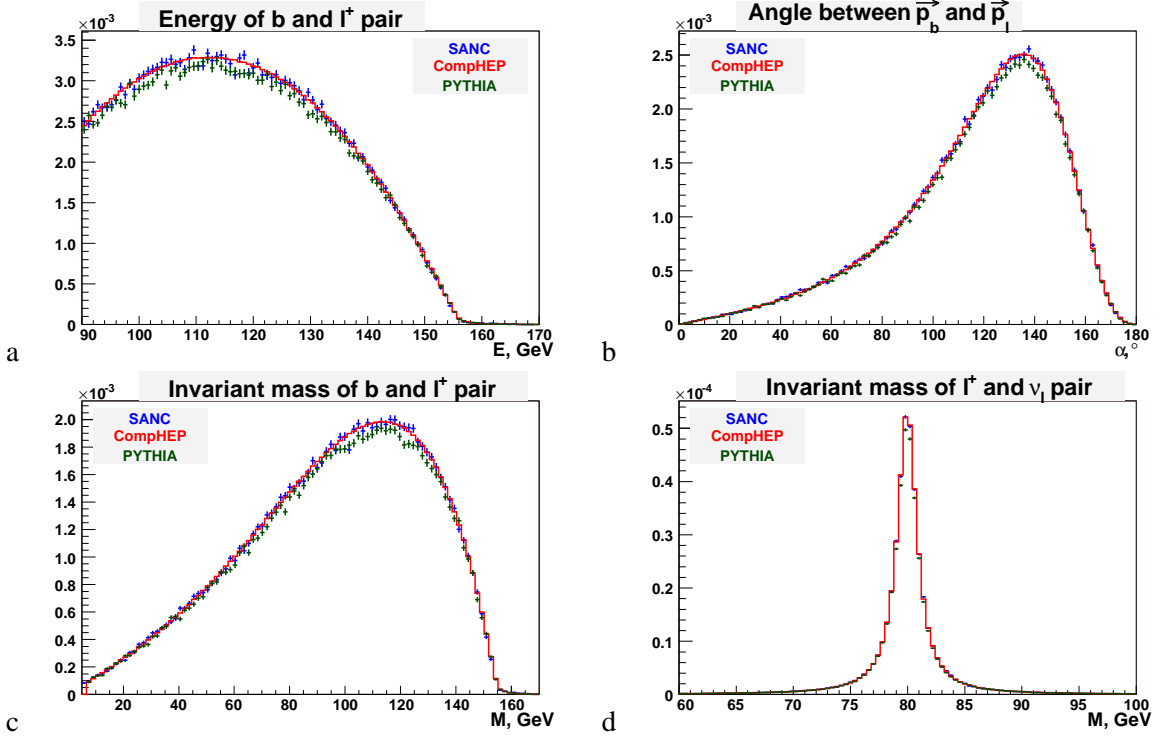


**Figure 2:** Differential distributions for Born-level process  $t \rightarrow b\mu^+ \nu_\mu$  produced by SANC, CompHEP and PYTHIA packages.

#### 4. Radiative corrections

Radiative corrections can be subdivided into three parts: hard-photon emission, soft photon emission and virtual (one-loop) corrections. Soft contribution is proportional to the Born-level decay rate and have the same phase space. Hard process  $t \rightarrow b + l^+ + \nu_l + \gamma$  have four-body phase space. An auxiliary parameter  $\bar{\omega}$  separates hard and soft photon regions.

##### 4.1 Hard photon contribution

For hard photon emission there are four tree-level Feynman diagrams (see Fig. 3). One diagram corresponds to emission from the initial state, two diagrams describe the final state radiation and remaining diagram corresponds to radiation from intermediate  $W^+$  boson.

Differential decay rate for hard process is represented by 5-fold integral:

$$\Gamma^{\text{hard}} = \int_{\Omega} ds_{25} ds_{34} d\cos\theta_1 d\cos\theta_2 d\phi_2 f(s_{25}, s_{34}, \cos\theta_1, \cos\theta_2, \phi_2). \quad (4.1)$$

Kinematics and meanings of variables are illustrated in Fig. 4. The results of Monte-Carlo integration are presented in Tab. 2.

There is a significant difference between two sets of numbers and this difference increases with decreasing of  $\bar{\omega}$  parameter. This difference is due to the approximation which implemented in CompHEP package for the representation of  $W$  boson propagators. CompHEP represents the

complex function for propagator as a real one:

$$\frac{1}{p^2 - m_W^2 + im_W \Gamma_W} \rightarrow \frac{p^2 - m_W^2}{(p^2 - m_W^2)^2 + m_W^2 \Gamma_W^2}. \quad (4.2)$$

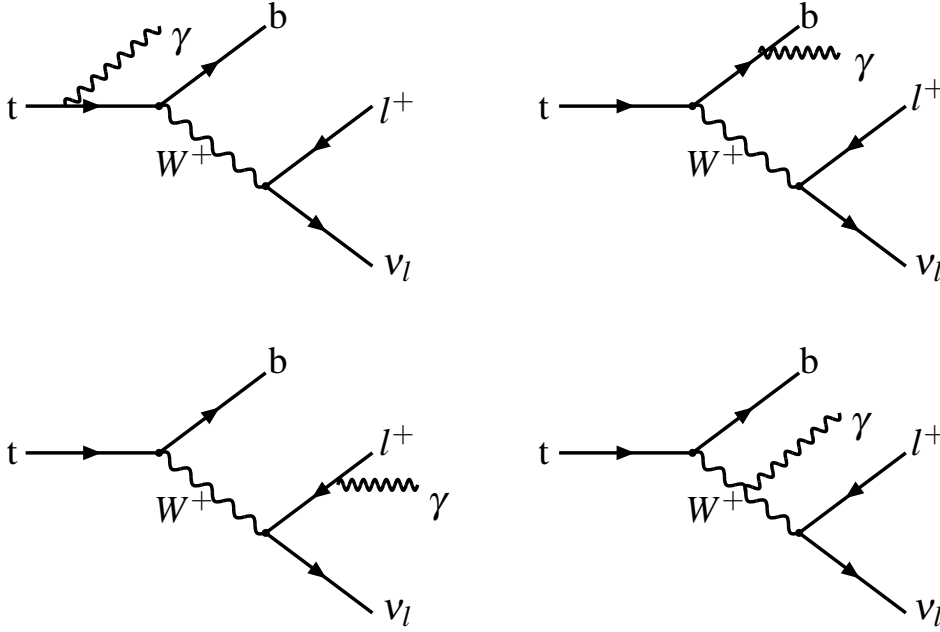


**Figure 3:** Feynman diagrams for the hard photon emission.

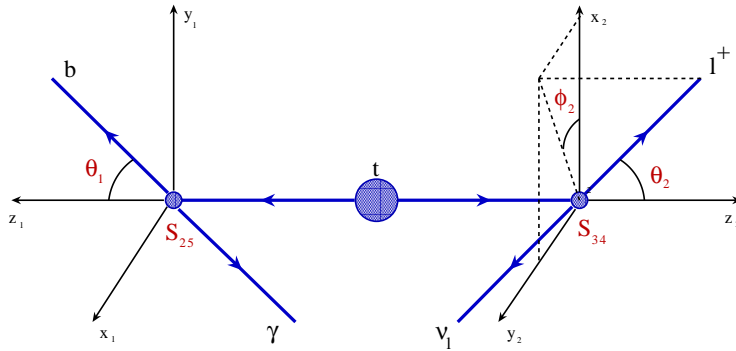


**Figure 4:** Kinematical diagram for the hard photon emission.

This assumption will not lead to noticeable departure from right result with the exception of the case when we have the product of two different W propagators. In this case it is necessary to make substitution that corrects this assumption:

$$\frac{p_1^2 - m_W^2}{(p_1^2 - m_W^2)^2 + m_W^2 \Gamma_W^2} \frac{p_2^2 - m_W^2}{(p_2^2 - m_W^2)^2 + m_W^2 \Gamma_W^2} \rightarrow$$

$$\frac{p_1^2 - m_W^2}{(p_1^2 - m_W^2)^2 + m_W^2 \Gamma_W^2} \frac{p_2^2 - m_W^2}{(p_2^2 - m_W^2)^2 + m_W^2 \Gamma_W^2} + \frac{M_m^2 \Gamma_W^2}{((p_1^2 - m_W^2)^2 + m_W^2 \Gamma_W^2)((p_2^2 - m_W^2)^2 + m_W^2 \Gamma_W^2)}. \quad (4.3)$$

$\bar{\omega}$ , GeV	$\Gamma^{\text{hard}}$ , $10^{-2}$ GeV (CompHEP)	$\Gamma^{\text{hard}}$ , $10^{-2}$ GeV (SANC)
10	0.2578(2)	0.2592(2)
1	0.6982(3)	0.8582(2)
$10^{-1}$	0.8538(3)	1.5000(3)
$10^{-2}$	0.9628(4)	2.1495(3)
$10^{-3}$	1.0730(4)	2.8005(4)
$10^{-4}$	1.1809(3)	3.4525(4)

**Table 2:** Comparison for hard emission produced by SANC and CompHEP systems.

We can explicitly observe the difference in Fig 5, where are presented the various differential distribution. As indicated in the upper two pictures the difference is to be observed in the region of soft photons and near the resonance.

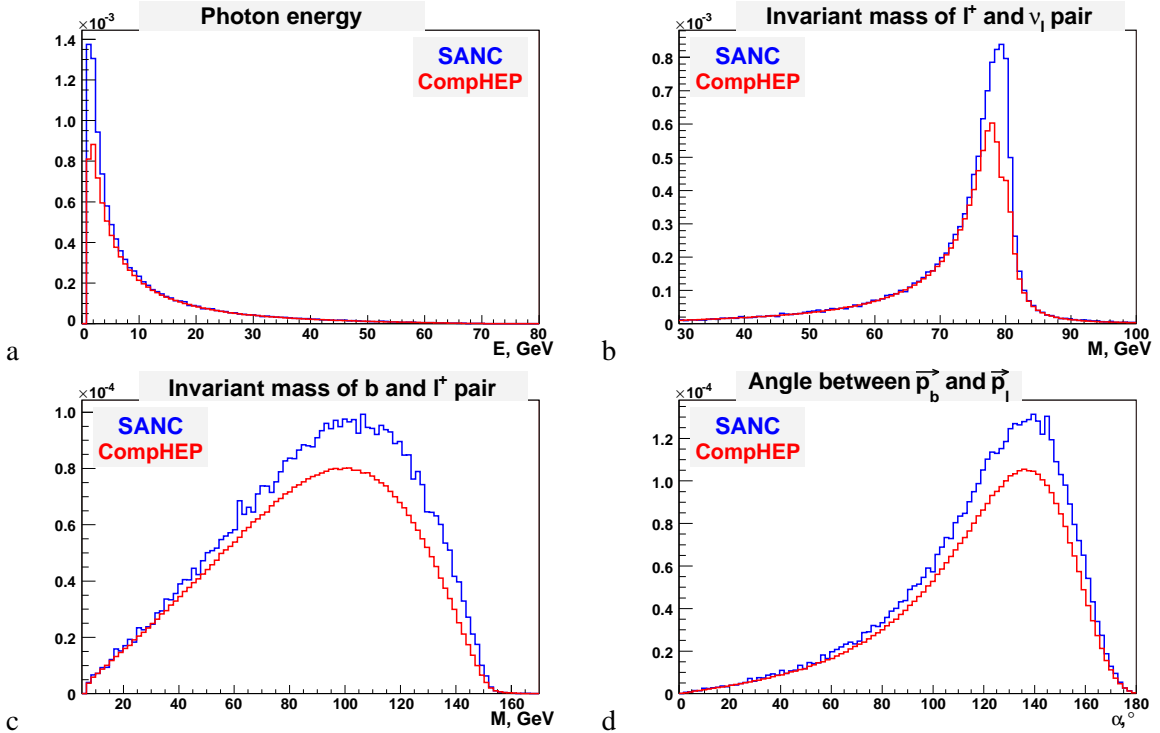


**Figure 5:** Differential distributions for the hard photon emission process  $t \rightarrow b \mu^+ \nu_l \gamma$ .

## 4.2 Soft and virtual corrections

In the automatized system the soft and virtual corrections are accessible via menu chain **SANC**  $\rightarrow$  **EW**  $\rightarrow$  **Processes**  $\rightarrow$  **4 legs**  $\rightarrow$  **4f**  $\rightarrow$  **Charged current**  $\rightarrow$  **t -> b l nu**  $\rightarrow$  **t -> b l nu (FF)**, see Fig. 6. The module, loaded at the end of this chain computes on-line the scalar form-factors of the decay process. The parallel module t -> b l nu (HA) provides the relevant helicity amplitudes. For more detail see section 2.5 of the SANC description [7] and the book [16].

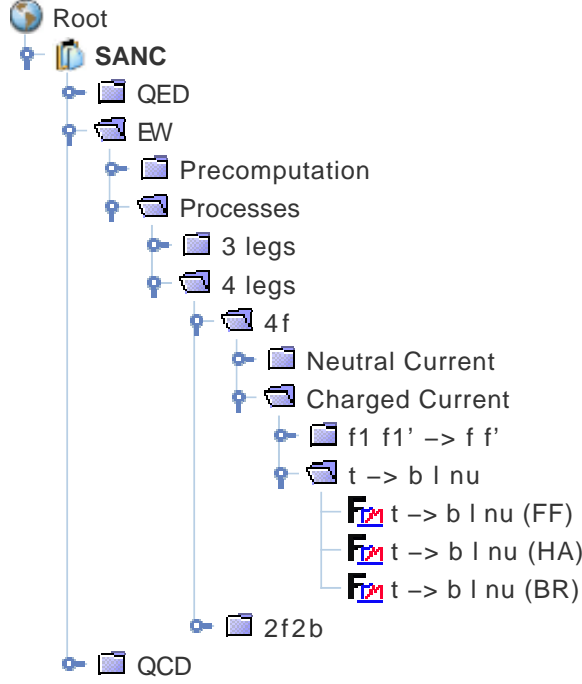


**Figure 6:** SANC tree for  $t \rightarrow bl^+ \nu_l$  decay.

## 5. Numerical results

The results of total 1-loop width calculation for  $\alpha$  and  $G_F$  scheme and comparison with Born level widths are presented in tables 3 and 4.

lepton	$\Gamma^{\text{Born}}, \text{GeV}$	$\Gamma^{1\text{-loop}}, \text{GeV}$	$\delta, \%$
$e^+$	0.16192(1)	0.17271(1)	6.66
$\mu^+$	0.16192(1)	0.17271(1)	6.66
$\tau^+$	0.16192(1)	0.17270(1)	6.66

**Table 3:** The results of the decay width computation in  $\alpha$  scheme.

lepton	$\Gamma^{\text{Born}}$ , GeV	$\Gamma^{1\text{-loop}}$ , GeV	$\delta$ , %
$e^+$	0.17302(1)	0.17527(1)	1.29
$\mu^+$	0.17303(1)	0.17527(1)	1.29
$\tau^+$	0.17303(1)	0.17526(1)	1.29

**Table 4:** The results of the decay width computation in  $G_F$  scheme.

## 6. Conclusion

A study of the semileptonic top quark decay  $t \rightarrow bl^+ \nu_l(\gamma)$  was presented. We computed total one-loop electroweak corrections to this process with help of the SANC system. Using Monte-Carlo integrator and events generator that were created we specify the decay width due to radiative corrections. These corrections are about 6.7% for  $\alpha$  scheme and approximately 1.3% for  $G_F$  scheme. The comparison with the numbers of CompHEP and PYTHIA packages was done at the tree level. During this comparison we found noticeable deviation from the CompHEP package for hard-photon emission in the region of resonance.

## Acknowledgments

This work was partially supported by the INTAS grant 03-41-1007 and by the RFBR grant 04-02-17192.

## References

- [1] S. M. Oliveira, L. Brucher, R. Santos, A. Barroso, *Electroweak corrections to the top quark decay*, Phys. Rev. D64: 017301, 2001 [hep-ph/0011324].
- [2] H. S. Do, S. Groote, J. G. Korner, M. C. Mauser, *Electroweak and finite width corrections to top quark decays into transverse and longitudinal W bosons*, Phys. Rev. D67: 091501, 2003 [hep-ph/0209185].
- [3] T. Kuruma, *Electroweak radiative corrections to the top quark decay*, Z. Phys. C57: 551-558, 1993.
- [4] B. Lampe, *Forward-backward asymmetry in top quark semileptonic decay*, Nucl. Phys. B454: 506-526, 1995.
- [5] *ATLAS detector and physics performance Technical Design report*, Volume II, 1999.
- [6] Q.-H. Cao, C.-P. Yuan, *Combined effect of QCD resummation and QED radiative correction to W boson observables at the Tevatron*, Phys. Rev. Lett. 93: 042001, 2004 [hep-ph/0401026].
- [7] A. Andonov, et al., *SANCscope - v. 1.00*, to appear in Comput. Phys. Commun. [hep-ph/0411186]; and references therein.
- [8] E. Boos, et al. (CompHEP Collaboration), *CompHEP 4.4: Automatic computation from Lagrangians to events*, Nucl. Instrum. Mech. A534 (2004), p250 [hep-ph/0403113].
- [9] T. Sjostrand, L. Lonnblad, S. Mrenna, P. Skands, *PYTHIA 6.3 physics and manual*, LU TP 03-38, 2003 [hep-ph/0308153].
- [10] D. Bardin, et al., *SANCnews: QCD sector*, in preparation.



- [11] M. Fischer, S. Groote, J. G. Korner and M. C. Mauser, *Complete angular analysis of polarized top decay at  $O(\alpha_s)$* , Phys. Rev. D65: 054036, 2002 [hep-ph/0101322].
- [12] M. Slysarczyk, *Two-loop QCD corrections to top quark decay*, Lake Louise 2004, Fundamental interactions, 284-288 [hep-ph/0401026].
- [13] B. H. Smith, M. B. Voloshin. *Normalization of QCD corrections in top quark decay*, Phys. Lett. B340, 176-180 (1994) [hep-ph/9405204].
- [14] S. Mrenna, C. P. Yuan, *QCD radiative decay of the top quark produced in hadron colliders*, Phys. Rev. D46, 1007-1021 (1992),
- [15] G. P. Lepage, *A new algorithm for adaptive multidimensional integration*, Journal of Computational Physics 27, 192-203, (1978).
- [16] D. Bardin, G. Passarino, *The Standard Model in the Making: Precision Study of Electroweak Interactions*, Oxford, Clarendon, 1999.